Journal of
Ceramic Science
and Technology

J. Ceram. Sci. Technol., **13** [2] 107-112 (2022)
DOI: 10.4416/JCST2022-00005
available online at: http://www.ceramic-science.com

Effect of Al_2O_3 Doping on Damping Properties of YSZ Coatings

G.Y. Du*[1], Y.T. Liu[1], G.H. Li[1], Y.S. Ni[1], X.Y. Liang[1], Z.L. Chen[1]

[1]School of Mechanical Engineering & Automation, Northeastern University, Shenyang 110819, China
received May 24, 2022; received in revised form October 19, 2022; accepted October 20, 2022

Abstract

In this paper, the changes in the microstructure and damping performance of x wt% Al-doped 8YSZ (xAl-YSZ, x = 0, 2.5, 5, 10, or 15) were investigated. Al-YSZ coatings with a thickness of about 80 µm were prepared on nickel-based alloys by means of EB-PVD. The surface morphology, phase composition and loss factor of the coatings were compared and analyzed by means of SEM, XRD, DMA, and SEM. XRD revealed that the grain size of the coating decreases, the preferred orientation changes to multi-orientation, and the diffraction peak intensity decreases. With reference to the DMA test results, it could be shown that doping an appropriate amount of Al_2O_3 improved the grain boundary density, while multi-orientation formed more interfaces and pores between grains, which makes the coating consume more energy as a result of internal friction under external load. Too much or too little doping was not conducive to improving the damping performance. The results indicate a direct influence of the Al_2O_3 content (up to 5 wt%) on the improvement of the damping performance.

Keywords: Al-YSZ, damping, doping property, damping performance, microstructure

I. Introduction

With the development of aviation technology, further improvement of the performance of aeroengines requires a higher inlet temperature and thrust weight ratio. It poses new challenges for the reliability of key components such as engine blades. The question of how to improve the fatigue damage resistance of key components such as blades under severe working conditions, such as high temperature and high load, has attracted more and more attention [1–3]. At present, passive vibration suppression techniques such as damping coatings are usually used to reduce the vibration stress level. For the damping coating, viscoelastic materials and hard coatings are commonly used. Although the loss factor (Q^{-1}) of viscoelastic material is higher than that of hard coatings, it is difficult to use this effectively on engine blades and other parts because it is mainly composed of organic polymer materials and exhibits poor stability in high-temperature environments [4]. It has been shown that the hard coating damping technology represented by a metal matrix and ceramics can effectively reduce the vibration stress level of thin-walled components such as blades [5,6]. Among them, an Yttria-Stabilized Zirconia (YSZ) coating has often been used as a thermal barrier coating because of its good thermal insulation, thermal shock resistance, corrosion resistance and other properties. Some studies have shown that it has certain vibration suppression ability and damping characteristics [7–9]. It can therefore be used as a multifunctional coating on engine blades and other parts.

At present, research on YSZ coatings has focused mainly on changing the process parameters in the preparation process and doping modification to improve the thermodynamic properties of the coating. For example, adding Al_2O_3, Gd_2O_3, CeO_2 and other materials to YSZ can improve the thermal insulation capacity [10,11]. Al_2O_3-YSZ has attracted the attention of scholars because of its excellent properties. A Al_2O_3 coating exhibits good strength, corrosion resistance and insulation performance. It is commonly used in wear-resistant coatings, insulation coatings as well as in other fields. Al_2O_3 may form unstable cubic phase in the spraying process (γ-Al_2O_3). And it has a low coefficient of thermal expansion, so it is not generally used directly as a raw material for thermal barrier coatings. The melting point of Al_2O_3 is 2 040 °C. During the spraying process, the melting state of Al_2O_3 is excellent, which can make the structure of the prepared coating more compact; the melting point of ZrO_2 is 2 700 °C, but its coefficient of thermal expansion is higher than that of Al_2O_3. The properties of YSZ and Al_2O_3 are complementary. It is a new idea to improve the performance of thermal barrier coatings to obtain composite materials by means of doping modification. So, there has been lots of studies on the mechanical properties, heat insulation ability, corrosion resistance of Al-YSZ coatings. Song Xuemei *et al.* found that doping Al_2O_3 can enhance the phonon scattering and reduce the thermal conductivity of the coating, and it can be used to prepare a thermal barrier coating that can work stably at 1 200 °C[12]. Chang *et al.* found that the Al-YSZ composite coating had a longer service life and thinner TGO layer by comparing the constant temperature oxidation test results of YSZ and Al_2O_3-YSZ[13]. Fariba *et al.* reported Al_2O_3 could prevent the phase transformation of tetragonal phase in 60 wt% Al-YSZ composite

* Corresponding author: gydu@mail.neu.edu.cn

coating [14]. At the same time, the crystallization of the amorphous phase in the coating can produce rich nano-regions, blocking the inward migration of air and the deflection of cracks. Yu *et al.* also inhibited the grain growth of ZrO_2 phase by adding nano Al_2O_3, thus improving the thermal stability of the coating [15]. With the doping of Al_2O_3, more oxygen vacancies and lattice distortion can be introduced into YSZ lattice, and these lattice defects can exist in the form of defect clusters. A large number of defects can aggravate the scattering of phonons in the material and reduce the average free path of phonons, so as to reduce the thermal conductivity of the coating. Some scholars have compared the corrosion resistance of YSZ and 40 wt% Al-YSZ to molten corrosion (Na_2SO_4, V_2O_5), and found that the failure time of Al-YSZ was 10 hours longer than that of YSZ [16,17]. At the ultra-high temperatures of 1 500 °C and 1 700 °C, the Al element can also form a solid solution of t-ZrO_2, which can prevent phase transformation [18]. There have been many studies on the influence of Al_2O_3 doping on the thermal insulation performance of YSZ coatings [19–21]. But the influence of Al_2O_3 doping on the change in the damping performance of the coating remains to be studied. The objective of this study was to investigate the influence of different amounts of Al_2O_3 on the damping performance of coatings. YSZ coatings doped with different contents of Al_2O_3 were prepared on Ni-based alloy by means of electron beam physical vapor deposition (EB-PVD). By comparing the samples with different doping amounts, with regard to the aspects of surface morphology, the phase composition and combined with the results of loss factor, this paper analyzes the influence of different doping amounts of Al_2O_3 on the change in the damping factor of YSZ coatings, and discusses the influence of Al_2O_3 doping modification on the damping characteristics of coatings. The purpose of the investigation is to provide a theoretical basis for optimizing the damping performance of coatings and preparing multifunctional composite coatings in the future.

II. Experimental

(1) Preparation of composite coatings

During the preparation of the coating, the substrates were Ni-based superalloy (GH4169) with the original size measuring 20 × 20 × 2 mm. Before the coating, the surfaces of the Ni-based alloy were sandblasted, wiped with alcohol and cleaned ultrasonically. The NiCoCrAlY adhesive layer was prepared with a thickness of 100 – 110 μm with flame-spraying equipment (QHT-7). The spraying distance was about 200 mm. The ceramic coating material was made of 8-wt% yttria-stabilized zirconia (99.99 %, Institute of Mining and Metallurgy, Beijing General Research Institute of Nonferrous Metals)particles with a diameter of 3 mm, and the Al_2O_3 used consist of amorphous powder (98 %, Sinopharm Chemical Reagent Co., Ltd). The composition of each group of materials is shown in Table 1. YSZ coatings were prepared by means of electron beam evaporation (EB-PVD) with a DSZ 700 electron beam evaporation coater. According to the preliminary experiment, when the working environment was 1×10^{-3} Pa in the vacuum state, the substrate temperature was 300 °C, the current of electron beam was 300 MA. The thickness of the ceramic layer was about 80 μm when the coating time was 30 minutes.

Table 1: Experimental raw materials for coating preparations.

Number	Experimental material	Substrates
1	8 wt%YSZ	Ni based-alloy
2	8 wt%YSZ+2.5 wt%Al_2O_3	Ni based-alloy
3	8 wt%YSZ+5 wt%Al_2O_3	Ni based-alloy
4	8 wt%YSZ+10 wt%Al_2O_3	Ni based-alloy
5	8 wt%YSZ+15 wt%Al_2O_3	Ni based-alloy

(2) Coating characterization test

The surface topography was characterized with an Ultra-plus scanning electron microscope with magnification of 20 ~ 300 000 times, and the local phase of the samples was analyzed with an X'pert Pro MPO diffractometer (XRD) with Cu ray. The working temperature was from room temperature to 900 °C, and the scanning range was 0.2° ~ 150°. The phase and microstructure of five groups of coating samples were analyzed.

The storage modulus (E′) and loss modulus (E″) of the samples were measured by means of the three-point bending method with a dynamic mechanical analyzer (DMA Q800), and the loss factor (Q^{-1}) was calculated according to Eq.(1) as follows, so as to evaluate the damping performance of the material. The scanning range of the DMA test frequency was 0.01 ~ 200 Hz. The amplitude range is 0.001 ~ 0.02 mm.

$$Q^{-1} = \frac{E''}{E'} \quad (1)$$

III. Results and Discussion

(1) Microstructure of the composite coatings

Fig. 1 shows the microstructure of the composite coatings doped with different proportions of Al_2O_3. When Al_2O_3 was not added, the surface morphology presented an elliptical stacking structure, and the gaps between different clusters were small. After the addition of 2.5 wt% Al_2O_3, the cluster shape became more rounded, the size decreased, and the boundary of spherical clusters was blurred. As the Al_2O_3 was mixed in the raw material, the melting point of the composite material in the crucible was reduced. While the electron beam current remained unchanged, the melting amount of material in the crucible increased in unit time, which formed a relatively smooth surface. With the increase in doping content, the cluster size further decreased and the distance between clusters increased. This is because the solid solubility of Al_2O_3 in YSZ is limited. A small amount of Al_2O_3 infiltrates into the lattice of ZrO_2 to form a solid solution, which plays a role in stabilizing t-ZrO_2. Al_2O_3 without solid solution forms amorphous phase on the grain boundary, which limits the grain size [21]. Fig. 2 shows the average particle size of different samples. According to Fig. 2, compared

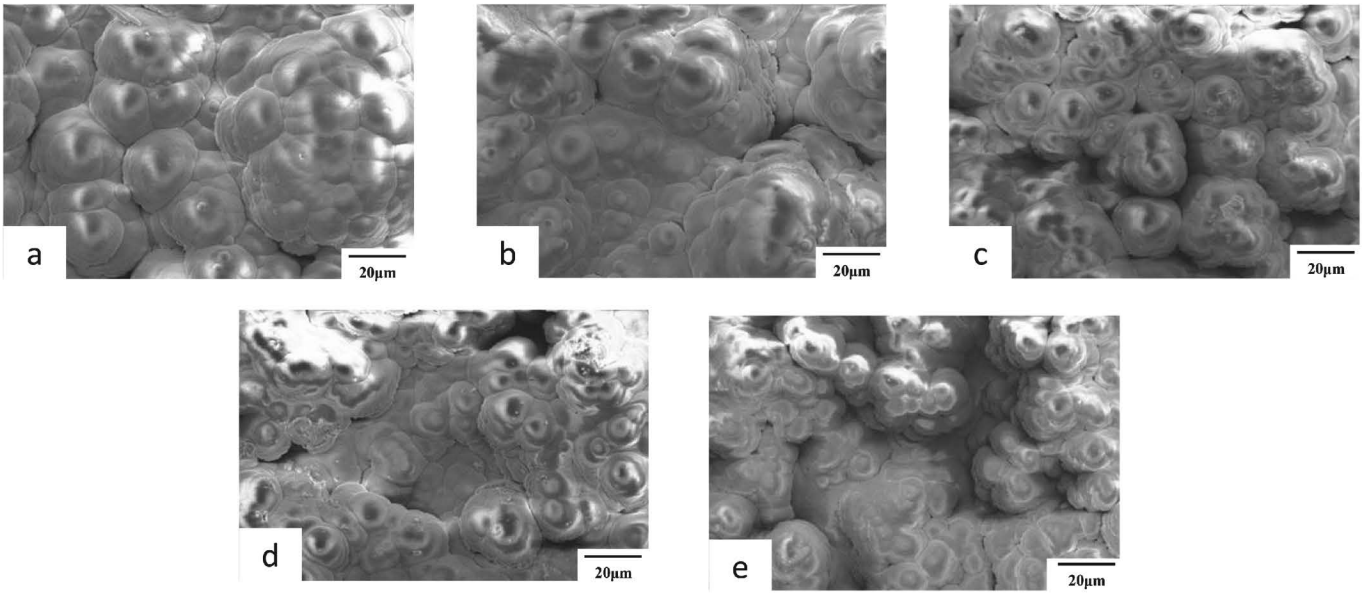

Fig. 1: Surface morphology of YSZ coatings doped with different Al_2O_3 contents a) 0 wt% b) 2.5 wt% c) 5 wt% d) 10 wt% e) 15 wt%.

with that before doping, the particle size is reduced by about one time (10 wt%, 15 wt%). When a small amount of alumina is introduced, the particle size will be significantly reduced, but when the doping ratio is increased to more than 10 %, the effect will not be obvious. The circular sphere growing upward at the top of the cluster is a new nucleation position, and the number of nucleation points is higher than that of the undoped sample. From Fig. 6, it can be found that at the doping ratio of 5 wt%, the average loss factor was the highest, reaching 0.06902, which was an around 6.91% improvement compared with that of YSZ coating.

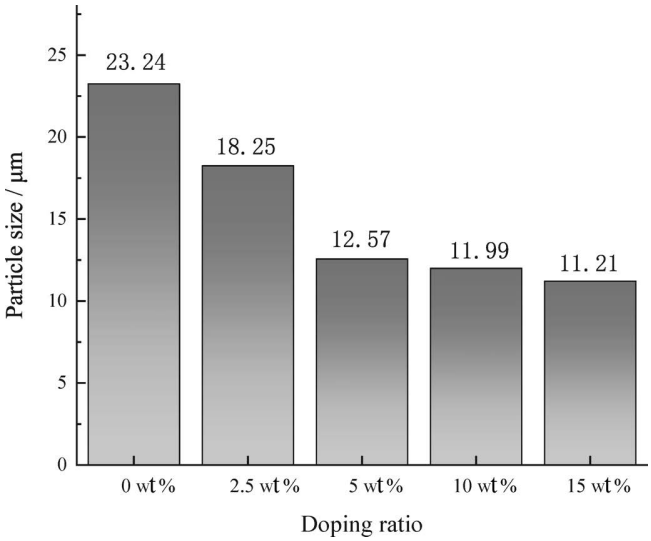

Fig. 2: Particle size of different samples.

(2) Coating phase analysis

An XRD diffractometer was used to observe the effect of different proportion of Al_2O_3 on the crystal structure of the coating. Fig. 3 shows the XRD pattern of different samples doped with 0 wt%, 2.5 wt%, 5 wt%, 10 wt%, and 15 wt% Al_2O_3. When Al_2O_3 was not added, the main component of the coating was t-ZrO_2, and the dominant direction was (101).With the addition of Al_2O_3, the peak value of the coating decreased significantly, and the preferred orientation changed significantly, evolving from a single preferred orientation to a mixed orientation dominated by (101) and (110).With the gradual increase of doping amount, the strength of all phases decreased, especially for (101) and (110). The proportion of (110) crystal direction gradually increased, and the crystal phase became more complex. The images with Al_2O_3 addition of 5 wt% and 10 wt% were basically the same, indicating that the crystal direction in this interval was relatively stable. However, when the doping amount was increased to 15 wt%, the intensity of all phases decreased, and the diffraction curve showed a large envelope peak shape without obvious characteristic peak. That is because there was too much melting of the material per unit time, and the columnar crystals on the coating surface are covered by the molten YSZ before they fully grown. Therefore, the crystal direction was chaotic. It was amorphous phases. In a comparison of the diffraction curves of samples with different doping amounts, it was found that the diffraction peak shifted toward a higher 2θ angle and then toward a lower 2θ angle. This trend is consistent with that in the relevant literature [12]. By XieLe formula ($2d\sin\theta = n\lambda$), it can be seen that the lattice constant decreases first and then increases. The decrease in the lattice constant is due to make the substitution of Zr^{4+} (0.079 nm) by Al^{3+} (0.054 nm) with smaller ion radius after the initial addition of Al_2O_3; with the increase of the proportion of doped Al_2O_3, part of Al^{3+} occupies the gap position of ZrO_2 lattice, resulting in the expansion of the lattice due to the narrow gap. No clear diffraction peak of Al can be observed in the XRD results, but the shift of the diffraction peak can be observed. It confirms that except for a few Al elements distributed outside the ZrO_2 lattice, most of the alumina exists in the form of amorphous phase.

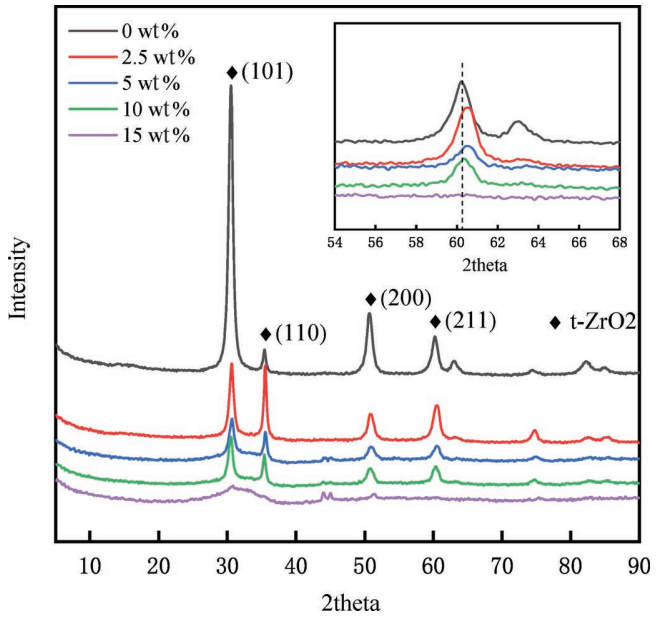

Fig. 3: XRD patterns of Al-YSZ samples for different percentages of Al_2O_3.

(3) Damping performance analysis

Fig. 4 (a) (b) shows the relationship between the storage modulus and loss modulus of the YSZ coatings with different Al_2O_3 doping. The storage modulus of the coating increased obviously when the content of alumina was 5 wt% and 10 wt%, but decreased when the content was too low. From the increase of the loss modulus curve (≥ 5 wt%), it can be seen that the loss modulus of the film increased significantly with the addition of Al_2O_3, which indicated that the surface of the coating had more micro defects. The energy consumption mechanism of ceramic coating was based mainly on the internal friction consumption of micro interfaces [21]. With the premise of not losing mechanical properties, the increase of micro defects helped to improve the damping capacity of the coating.

A DMA dynamic tester was used to test the samples with different doping ratios. The damping performance of the samples was characterized by the value of loss factor (Q^{-1}). Fig. 5 shows the loss factor of different samples. The difference in the damping factor among the samples is not significant when the strain is lower than 0.012 %. In the range of more than 0.012 %, the curve slope of the coating doped with Al_2O_3 is significantly greater than that of the undoped control group. The loss factor of the coating doped with Al_2O_3 was significantly improved under the same strain. The addition of Al_2O_3 made the microstructure and phase composition of the coating change obviously. Different from other groups, when the doping ratio was 2.5 wt%, the damping performance of the composite coating decreased, because the denser alumina blocks the pores, reduces the number of micro defects in the coating, and leads to the degradation of damping performance. When the doping ratio was 5 wt%, the decrease in grain size increases the grain boundary density. These grain boundaries exhibit viscous behavior, and relaxation phenomenon occurs under the action of exciting force. The coating with mixed orientation has a shadow effect and contains more micro voids, which can improve energy dissipation through internal friction during vibration. Combined with the morphology of the coating, when the doping amount was low, the doping of Al_2O_3 changed the original lattice constant, and the grains of the coating became rounder and easier to agglomerate. This led to the blurring of grain boundary and the decrease of grain boundary density, which reduced the damping performance. With the increase of doping content, the grain size decreased and the distance between clusters increased. This trend led to more grain boundaries in the film. Under the action of excitation force, the relaxation phenomenon of the boundary made the boundary consume more energy during friction, which improves the damping performance of the coating [22]. Combined with the phase analysis of the coating, the peak value of the coating gradually decreases and the preferred orientation also changes. In the XRD image, the prominent main peak represents the orderly arranged grains. After doping, the decreasing trend of the

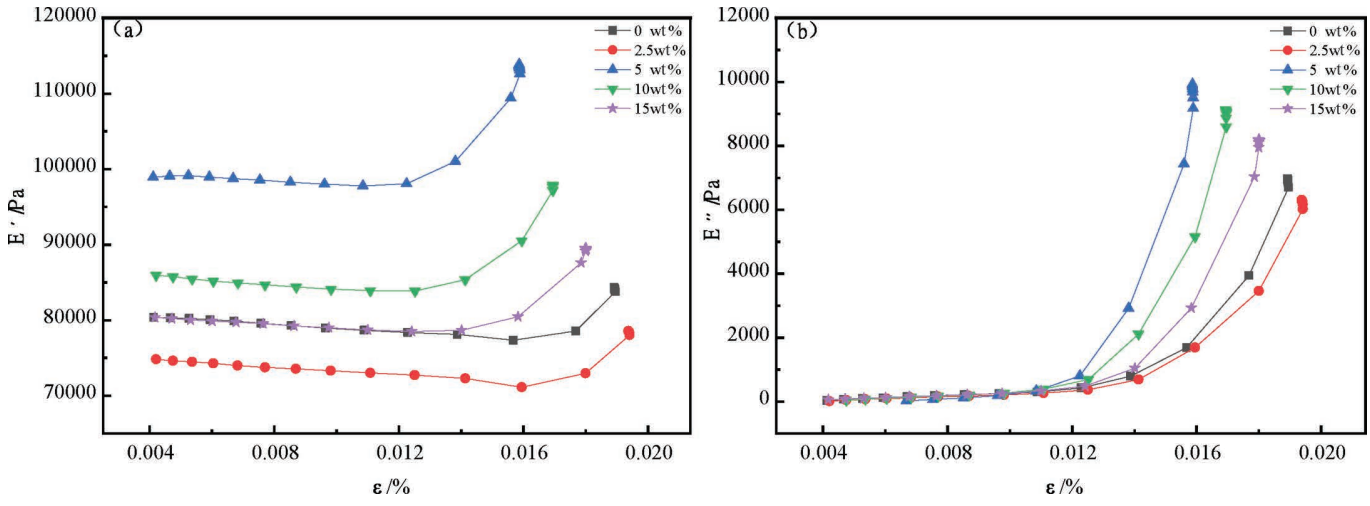

Fig. 4 (a): Relationship between storage modulus (E') and strain; (b): Relationship between loss modulus (E'') and strain.

main peak intensity indicates that the grains are becoming gradually finer while grain growth is becoming increasingly disordered, which can help to improve the damping performance of the coating [23–26].

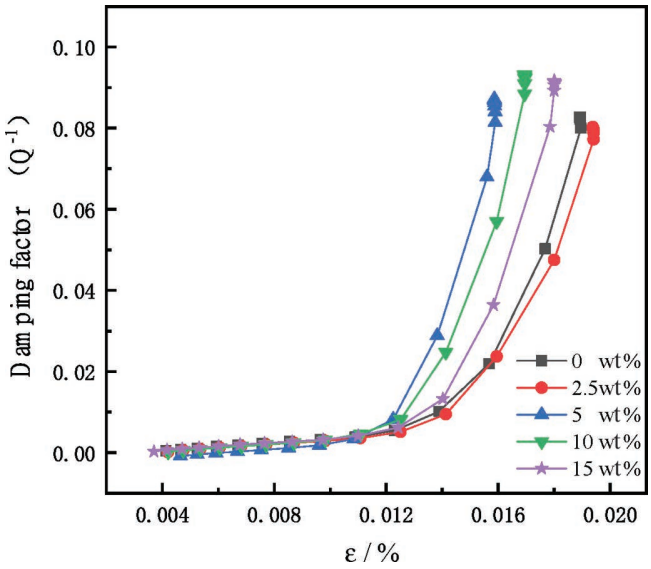

Fig. 5: Relationship between loss factor and strain.

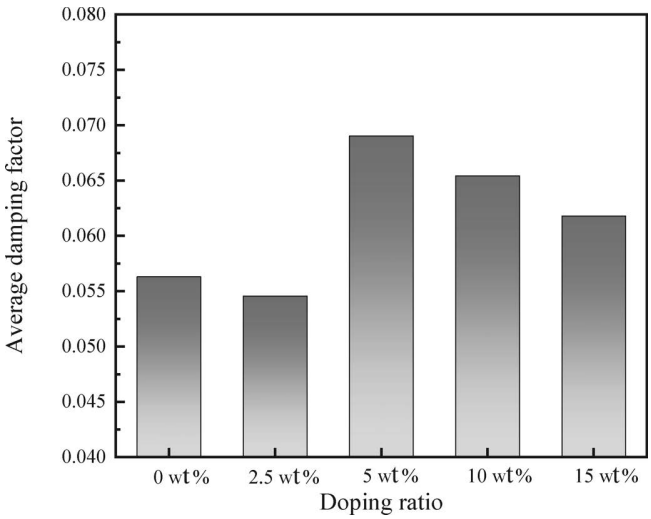

Fig. 6: Average damping factor of each group.

Acknowledgment

This work was financially supported by Funds for Basic Scientific Research Funds for Central Universities [grant number N2203020]. We also thank sci-go (www.sci-go.com) for their support in DMA test.

IV. Conclusions

In this paper, YSZ coatings doped with different proportions of Al_2O_3 were prepared on the surface of Ni-based alloy by means of electron beam evaporation. The conclusions are as follows:

1) Appropriate addition of Al_2O_3 can improve the loss factor of the coating, so the damping property of the YSZ coating is improved.
2) Following addition of Al_2O_3 into YSZ layer, the grain growth was inhibited by the Al_2O_3.The grain size of the coating decreases, the grain boundary density increases, the cluster spacing increases, and the preferred orientation changes from single orientation to mixed orientation. This increases the energy consumption during boundary friction, which improves the damping performance of the coating.
3) The doping ratio has an effect on the damping performance of the coating. When the doping amount is too low, the grain boundary becomes blurred; when the doping amount is too high, the coating is composed of amorphous phase. This is not conducive to improving the damping performance of the coating. When the doping ratio is 5 wt%, the damping performance of the YSZ coating is significantly improved.

References

1 Gao, J., Gao, Y., Yan, X.: Damping mistuning effect of the hard-coating-based intentional mistuning techniques on mistuned blisks and its mechanism, *Aerosp. Sci. Technol.*, **101**, 105848, (2020).

2 Bhaumik, S.K., Sujata, M., Venkataswamy, M.A., Parameswara, M.A.: Failure of a low pressure turbine rotor blade of an aeroengine, *Eng. Fail. Anal.*, **13**, 1202–1219, (2006).

3 Jiang, R., Song, Y.D., Reed, P.A.: Fatigue crack growth mechanisms in powder metallurgy Ni-based superalloys – A review, *Int. J. Fatigue.*, **141**, 105887, (2020).

4 Murota, N., Suzuki, S., Mori, T.: Performance of high-damping rubber bearings for seismic isolation of residential buildings in Turkey, *Soil Dyn Earthq Eng.*, **143**, 106620, (2021).

5 Paul, T., Nautiyal, P., Zhang, C.: Role of in-situ splat sintering on elastic and damping behavior of cold sprayed aluminum coatings, *Scripta Mater.*, **204**, 114–125, (2021).

6 Xu, K., Yan, X., Du, D.: Vibration response prediction of coated blisks under multi-point non-contact excitations using mistuning identification data, *Thin Wall Struct.*, **159**, 10732, (2021).

7 Patsias, S., Saxton, C., Shipton, M.: Hard damping coatings: an experimental procedure for extraction of damping characteristics and modulus of elasticity, *Mat. Sci. Eng. A-Struct.,*. **370**, [1–2], 412–416, (2004).

8 Limarga, A.M., Duong, T.L., Gregori, G., Clarke, D.R.: High-temperature vibration damping of thermal barrier coating materials, *Surf. Coat. Tech.*, **202**, [4–7], 693–697, (2007).

9 Yu, L.M, Ma, Y., Zhou, C.G., Xu, H.B.: Damping efficiency of the coating structure, *Int. J. Solid Struct.*, **42**, 3045–3058, (2005).

10 Wei, X.D., Hou, G.L., Zhao, D.: Recent research progress of oxide doped YSZ thermal barrier coatings, *Surf. Tech.*, **49**, [06], 92–103, (2002).

11 Lashmi, P.G., Balaji, N., Senthil Kumar, S.: Hot corrosion properties of plasma sprayed $La_2Ce_2O_7$/YSZ vis-à-vis $La_2Ce_2O_7$/cluster paired zirconia thermal barrier coatings, *Surf. Coat. Tech.*, **409**, 126902, (2021).

12 Song, X., Xu, Y., Ding, Y., Zhang, J.M., Guo, X., Jiang C.F., Zheng, W., Zeng, Y.: Study of microstructure, electronic structure and thermal properties of Al_2O_3-doped tetragonal YSZ coatings, *Appl. Surf. Sci.*, **542**,148553, (2021).

13 Chang, S.Y., Guo, X.X., Ni, X.J.: Optical Metasurfaces: Progress and Applications, *Annu. Rev Mater. Res.*, **48**, [1], 279–302, (2018).

14 Tarasi, F., Medraj, M., Dolatabadi A.: High-Temperature Performance of Alumina-Zirconia Composite Coatings Containing Amorphous Phases, *Adv. Funct. Mater.*, **21**, 4143–4151, (2011).

[15] Yu, Q.H., Zhou, C.G., Zhang, H.Y., Zhao, F.: Thermal stability of nanostructured 13 wt% Al_2O_3-8 wt% Y_2O_3-ZrO_2 thermal barrier coatings, *J. Eur. Ceram. Soc.*, **30**, [4], 889 – 897, (2010).

[16] Afrasiabi, A., Saremi. M., Kobayashi, A.: A comparative study on hot corrosion resistance of three types of thermal barrier coatings: YSZ, YSZ+Al_2O_3 and YSZ/Al_2O_3, *Mat. Sci. Eng. A-Struct.*, **478**, 264 – 269, (2008).

[17] Keyvani, A., Saremi, M., Sohi, M.H.: Microstructural stability of zirconia-alumina composite coatings during hot corrosion test at 1050 °C, *J. Alloy Compd.*, **506**, 103 – 108, (2010).

[18] Karvounis, A., Gholipour, B., Macdonald, K.F.: All-dielectric phase-change reconfigurable metasurface, *Appl. Phys. Lett.*, **109**, [051103], 1 – 5, (2016).

[19] Song, X., Zhang, J., Liu, Z., Jiang, C.F., Lin, C.C., Zeng, Y.: Thermal shock resistance of YSZ, YSZ-Al_2O_3 and YSZ-Al_2O_3/YSZ coatings, *Vacuum*, **162**, 150 – 155, (2019).

[20] Zhu, C., Javed, A., Li, P., Yang, F., Liang, G.Y., Xiao, P.: A study of the microstructure and oxidation behavior of alumina/yttria-stabilized zirconia (Al_2O_3/YSZ) thermal barrier coatings, *Surf. Coat Tech*., **212**, 214 – 222, (2012).

[21] Lu, F.Z., Liu, H.T., Huang, W.Z.: Research progress of 8YSZ-Al_2O_3 composite thermal barrier coating, *Mater. Rev*., **35**, [7], 42 – 47, (2018).

[22] Abu Al-Rub RK., Palazotto, A.N.: Micromechanical theoretical and computational modeling of energy dissipation due to nonlinear vibration of hard ceramic coatings with microstructural recursive faults, *Int. J. Solids Struct*., **47**, [16], 2131 – 2142,(2010).

[23] Du, G.Y., Tan, Z., Lin, Z.: Effect of ZrO_2 coating on substrate damping characteristics, *Northeast U. (Nat. Sci. Ed.)*., **39**, [10], 1501 – 1505, (2018).

[24] Shin, S., Kwon, M., Cho, W., Cho, W., Suh, I.S., De Cooman, B.C.: The effect of grain size on the damping capacity of Fe-17 wt% Mn, *Mat. Sci. Eng. A-Struct.*, **683**, 187 – 194, (2017).

[25] Nielsen, J., Jacobsen, T.: Three-phase-boundary dynamics at Pt/YSZ microelectrodes, *Solid State Ionics*., **178**, [13 – 14], 1001 – 1009, (2007).

[26] Krumov, E., Mankov, V., Starbova, K.: Nanosized columnar microstructure and related properties of electron gun deposited Al_2O_3 thin films, *Vacuum*, **76**, [2 – 3], 211 – 214, (2004).